

Synergistic Catalysis

Palladium Nanoparticles Bonded to Two-Dimensional Iron Oxide Graphene Nanosheets: A Synergistic and Highly Reusable Catalyst for the Tsuji–Trost Reaction in Water and Air

Jian Liu, Xing Huo, Tianrong Li, Zhengyin Yang, Pinxian Xi, Zhiyi Wang, and Baodui Wang^{*[a]}

Abstract: Low cost, high activity and selectivity, convenient separation, and increased reusability are the main requirements for noble-metal-nanocatalyst-catalyzed reactions. Despite tremendous efforts, developing noble-metal nanocatalysts to meet the above requirements remains a significant challenge. Here we present a general strategy for the preparation of strongly coupled Fe₃O₄ and palladium nanoparticles (PdNPs) to graphene sheets by employing polyethyleneimine as the coupling linker. Transmission electron microscopic images show that Pd and Fe₃O₄ nanoparticles are highly dispersed on the graphene surface, and the mean particle size of Pd is around 3 nm. This nanocatalyst exhibits

synergistic catalysis by Pd nanoparticles supported on reduced graphene oxide (rGO) and a tertiary amine of polyethyleneimine (Pd/Fe₃O₄/PEI/rGO) for the Tsuji–Trost reaction in water and air. For example, the reaction of ethyl acetoacetate with allyl ethyl carbonate afforded the allylated product in more than 99% isolated yield, and the turnover frequency reached 2200 h⁻¹. The yield of allylated products was 66% for Pd/rGO without polyethyleneimine. The catalyst could be readily recycled by a magnet and reused more than 30 times without appreciable loss of activity. In addition, only about 7.5% of Pd species leached off after 20 cycles, thus rendering this catalyst safer for the environment.

Introduction

Currently the design of multifunctional heterogeneous metal catalysts that preserve high metal dispersion and stability during the catalytic reactions and easily separate from the reaction mixture are of great importance. Noble-metal nanoparticles (NMNPs) with ultrafine size have attracted more and more attention owing to their superior catalytic activity in carbon–carbon cross-coupling, water splitting, methanol oxidation, and so forth.^[1] However, NMNPs with small particle size in the reaction conditions tend to aggregate and lose their catalytic activities.^[2] Moreover, the high cost and limited resources also hinder their practical application. To solve these problems, the particles are often immobilized on various solid supports, such as carbon materials, metal oxides, polymers, and so on.^[3] Among all solid supports studied thus far, magnetic nanoparticles^[4] and graphene^[5] have attracted particular interest because magnetic NPs have efficient magnetic separation capacity for easy separation of the catalyst from the reaction solution and graphene has a high surface area, which offers an effective

protocol to minimize aggregation and maximize the chemically accessible area. Despite numerous efforts to use magnetic NPs and graphene as supports for NMNPs for catalytic applications, an easily controlled architecture of magnetic NPs/graphene hybrid materials as a magnetically recoverable catalyst support on which NMNPs are covalently bonded by using a stabilizer and that exhibit high dispersion has not been synthesized and studied. Such ternary conjugates should serve as new multifunctional heterogeneous catalysts to enhance activity and stability, and accordingly, reduce their cost and minimize environmental contamination.

Given the rise of green chemistry, organic reactions conducted in water have received considerable attention since water is nontoxic, nonflammable, and the cheapest solvent in the world.^[6] Palladium allylic substitution, also called the Tsuji–Trost reaction, is a reliable and widely used method for carrying out C–C and C–O bond formation in organic syntheses.^[7] Usually, these reactions are carried out in organic and often toxic solvents. However, only a limited variety of supported palladium catalysts have been reported up to now for aqueous heterogeneous Tsuji–Trost reactions.^[8] The catalysts reported so far are recovered by tedious filtration or centrifugation, and the recycling of the catalysts has not been a consideration. Therefore, more efficient systems are still in demand.

In this study, we demonstrate an efficient and universal strategy for the in situ growth of palladium nanoparticles (PdNPs) and the assembly of Fe₃O₄ NPs on reduced graphene oxide (rGO) by employing polyethyleneimine (PEI) as the coupling linker among the three components. In these nanocomposites, GO could provide a large surface area on which the active

[a] J. Liu, Prof. X. Huo, Dr. T. R. Li, Prof. Z. Y. Yang, Prof. P. X. Xi, Z. Y. Wang, Prof. B. D. Wang
Key Laboratory of Nonferrous Metal Chemistry and Resources Utilization of Gansu Province and State Key Laboratory of Applied Organic Chemistry
Lanzhou University Gansu, Lanzhou, 730000 (P.R. China)
Fax: (+86) 931-8912582
E-mail: wangbd@lzu.edu.cn

Supporting information for this article is available on the WWW under <http://dx.doi.org/10.1002/chem.201402545>.

phase is finely dispersed and covalently anchored. These nanocomposites have a well-defined 2D morphology, confined PdNPs and Fe₃O₄ NPs in the PEI, controllable particle size, and high specific surface areas. Inspired by the monodisperse, ultrafine, and pristine properties of PdNPs on the same rGO surface as the tertiary amine of polyethyleneimine (Pd/Fe₃O₄/PEI/rGO), we sought to determine whether Pd/Fe₃O₄/PEI/rGO exhibits synergistic catalysis for the acceleration of the Tsuji–Trost reaction in water and air. The Pd/Fe₃O₄/PEI/rGO catalyst could be easily separated from the reactant with the simple application of an external magnetic field, and its catalytic efficiency was still high even after recycling 30 times in water.

Results and Discussion

Particle preparation and characterization

The overall synthetic strategy of Pd/Fe₃O₄/PEI/rGO nanocomposites is illustrated in Figure 1a. First, PEI was chemically modified on the GO surface by amide bonds, which led to the formation of PEI-grafted rGO (PEI/rGO). Second, the resulting PEI/rGO nanosheets were treated with 3,4-dihydroxybenzaldehyde (DIB) to introduce DIB onto rGO for the coordination assembly of Fe₃O₄ NPs.^[9] The resulting product was stirred with PdCl₂ in a solution of ethanol for two hours to ensure that the metal ion thoroughly bonded to the N atoms of the PEI. NaBH₄ was then added and stirred for one hour to generate PdNPs in situ.^[10] Finally, the obtained Pd/PEI/rGO composites were reacted with the as-synthesized Fe₃O₄ NPs to form Pd/Fe₃O₄/PEI/rGO. Surface catechol groups and amino groups therefore enhanced the stability and dispersity of Fe₃O₄ NPs and PdNPs on rGO, respectively.

The composition of Pd/Fe₃O₄/PEI/rGO nanocomposites was confirmed by FTIR. (Figure S2 in the Supporting Information). In the FTIR spectrum of Pd/Fe₃O₄/

PEI/rGO nanocomposites, the Pd–N absorption bands appeared at 624 cm⁻¹, and Fe–O absorption bands appeared at 594 and 445 cm⁻¹, respectively.^[11b] The above characteristics were also found for Pd/DIB/PEI/rGO and Fe₃O₄/DIB/PEI/rGO, respectively. These indicate that PdNPs and Fe₃O₄ NPs are conjugated by means of the DIB/PEI/rGO. Figure 1b–e shows the TEM images of the PEI/rGO, Pd/PEI/rGO, and Pd/Fe₃O₄/PEI/rGO

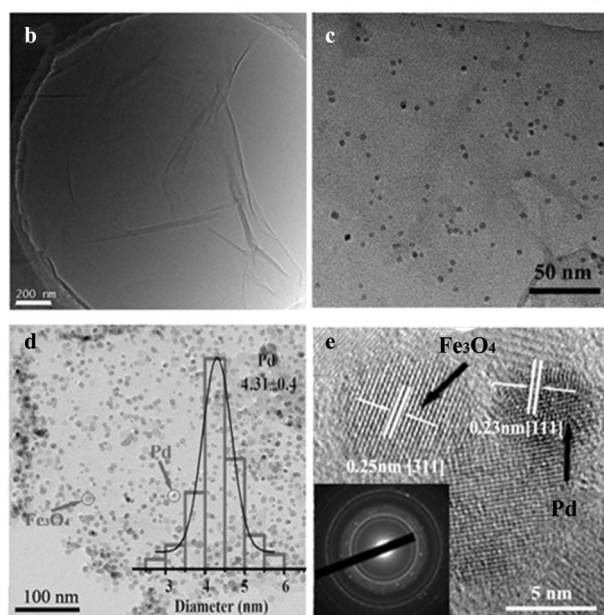
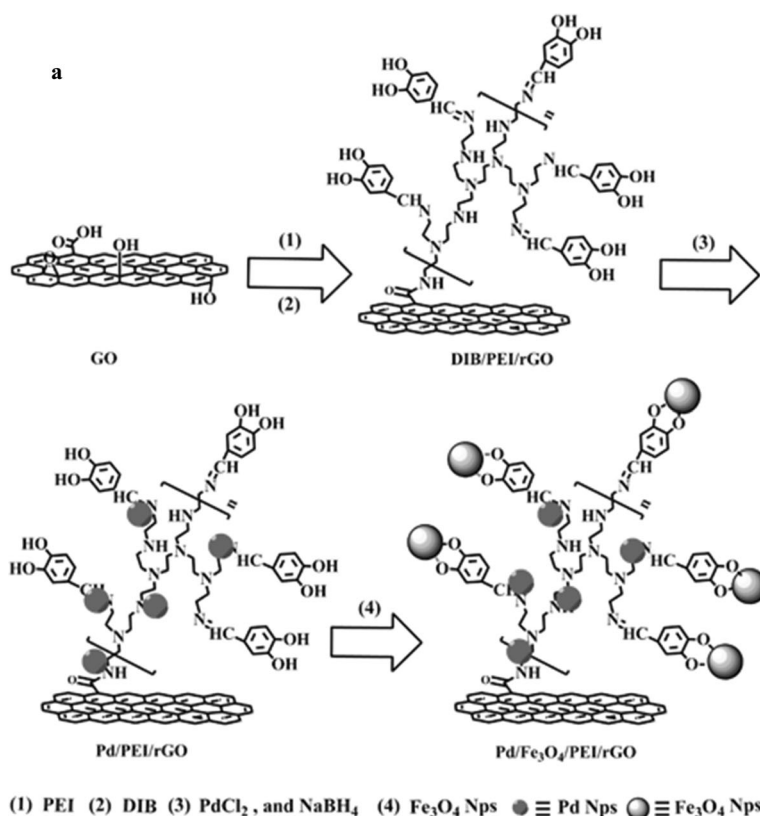


Figure 1. a) Synthetic route of Pd/Fe₃O₄/PEI/rGO. TEM images of b) PEI/rGO, c) Pd/PEI/rGO, and d) Pd/Fe₃O₄/PEI/rGO. The inset shows the nanoparticle size distribution of Pd at rGO. e) HRTEM image and the SAED pattern of Pd/Fe₃O₄/PEI/rGO nanocomposites.

nanohybrids. The monodisperse Fe₃O₄ NPs and the relatively uniform PdNPs were well dispersed on the surface of the rGO without clear aggregation. The morphology of Fe₃O₄ NPs was also unchanged after chemical modification onto rGO. The sizes of Pd particles are uniform, and the mean diameters are (4.31 ± 0.40) nm (inset of Figure 1d). The high-resolution TEM (HRTEM) image (Figure 1e) reveals that the Pd nanocrystals and Fe₃O₄ NPs are spherical with resolved lattice fringes.^[2,11] The selected-area electron diffraction (SAED) pattern (inset of Figure 1e) also confirms the presence of PdNPs and Fe₃O₄ NPs. The typical energy-dispersive X-ray (EDX) pattern (Figure S3 in the Supporting Information) indicates that the Pd/Fe₃O₄/PEI/rGO composites contain Pd, Fe, O, N, and C, whereas all of the elemental Cu and some of the C come from the carbon-coated copper grids. Inductively coupled plasma (ICP) results indicate that the loading capacities of the Pd on the magnetic support are 1.93 wt%, and the ratio of amine groups to Pd is 66:1.

Scanning TEM and an elemental mapping investigation of Pd/Fe₃O₄/PEI/rGO were performed to illustrate the distribution of carbon, nitrogen, palladium, iron, and oxygen components in the hybrids (Figure S4c–g in the Supporting Information). The C distribution appears to be uniform across the 2D nanosheets. The N and O distributions are similar to the C distribution but with a weaker energy-dispersive X-ray spectroscopy (EDS) signal. In contrast, the palladium and iron species are only identified within the nanometer-sized domains, which are homogeneously dispersed on the 2D nanosheets. These results imply that PdNPs and Fe₃O₄ NPs are formed in the polymer and not on the GO during the in situ growth and assembly,^[12] respectively, and the four components (PEI, Pd, Fe₃O₄, and graphene) are strongly coupled together in the nanocomposites.

The Pd/Fe₃O₄/PEI/rGO nanocomposites were also characterized by X-ray photoelectron spectroscopy (XPS) and powder X-ray diffraction (XRD) analysis. The sharp N and O peaks in Figure 2a and c demonstrate the presence of PEI, Fe₃O₄, and DIB in the Pd/Fe₃O₄/PEI/rGO nanocomposites. The XPS spectrum of Pd 3d can be fitted into a main doublet peak, as shown in Figure 2b. The binding energy of the doublet peaks at 335.4 eV (assigned to Pd⁰ 3d_{5/2}) and 340.7 eV (assigned to Pd⁰ 3d_{3/2}) can be attributed to the Pd⁰ state.^[2,13] Similarly, the XPS spectrum of the Fe 2p region (Figure 2c) clearly indicates that Fe₃O₄ NPs also exist on the PEI/rGO nanocomposites.^[11] Figure 2d shows the XRD pattern of the as-synthesized Pd/Fe₃O₄/PEI/rGO nanocomposites. The peaks located at 29.91, 35.41, 43.11, 57.21, and 62.81° (2θ) indicate the presence of Fe₃O₄.^[11] The weak peak appears around 2θ = 24°, which is the characteristic peak of residual unoxidized graphite.^[13] Moreover, new peaks that correspond to the (111) reflection of Pd crystal are observed for Pd/Fe₃O₄/PEI/rGO, thus reconfirming the successful growth of metal particles on the surface of magnetic hybrids again.^[2,3g]

The magnetic properties of the obtained samples were investigated by using a vibrating sample magnetometer (VSM) system at room temperature. The magnetization curves in Figure 2e show that Pd/Fe₃O₄/PEI/rGO nanocomposites are superparamagnetic at room temperature. The saturation magnetization values for Fe₃O₄ NPs and Pd/Fe₃O₄/PEI/rGO are 48.2 and 18.4 emu g⁻¹, respectively. The decrease in saturation magneti-

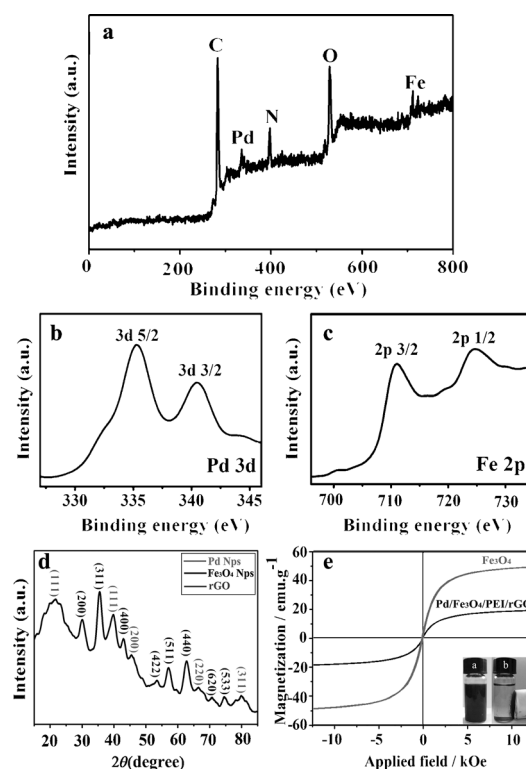


Figure 2. a) XPS spectra of Pd/Fe₃O₄/PEI/rGO. b) Spectrum in the Pd 3d region. c) Spectrum in the Fe 2p region. d) XRD pattern of Pd/Fe₃O₄/PEI/rGO. e) Magnetic behavior of Fe₃O₄ NPs and Pd/Fe₃O₄/PEI/rGO at 300 K. The photographs demonstrate that Pd/Fe₃O₄/PEI/rGO in aqueous solution can be attracted and arranged vertically by a magnetic bar.

zation is caused by the increasing amount of noble metal, PEI, and rGO in the hybrids. The photographs in Figure 2e demonstrate that the Pd/Fe₃O₄/PEI/rGO composites in aqueous solution can be harvested and separated by a magnetic field, which is important for the magnetic separation and reusability of the Pd/Fe₃O₄/PEI/rGO composites from the reaction mixture.

The Tsuji–Trost allylation of 1,3-dicarbonyl compounds with allyl ethyl carbonate

Recent societal demands to develop sustainable chemistry have increasingly led to chemists considering water as a benign solvent. Given that the Pd/Fe₃O₄/PEI/rGO catalyst is highly dispersed in water, we performed the Tsuji–Trost reaction in water and air. In a preliminary catalysis study, ethyl acetoacetate **1** as a model substrate with the allyl ethyl carbonate **2** as the nucleophile was chosen to optimize the reaction conditions (Table S1 in the Supporting Information). Herein, Pd/Fe₃O₄/PEI/rGO catalyst containing 1.8 μmol Pd was used in all the reactions if not stated otherwise. We screened various amounts of PPh₃ and found that 7.2 μmol PPh₃ (four times the amount of Pd) gave the corresponding diallylated products **4** in more than 99% yield in one hour (Table S1 of the Supporting Information, entry 3). A decrease in the temperature from 100 to 30 °C resulted in a lower yield (<10%) (Table S1 of the Supporting Information, entry 6). When PPh₃ was omitted, the

allylic alkylation yield was less than 41% (Table S1 of the Supporting Information, entry 1). When K_2CO_3 was used in this system in the absence of PPh_3 , 73% isolated yield was obtained (Table S1 of the Supporting Information, entry 8). However, in the presence of both K_2CO_3 and PPh_3 , the allylated product yield was 79% (Table S1 of the Supporting Information, entry 9). The low yield might be due to hydrolysis of ethyl acetoacetate **1** in basic conditions. Thus, Tsuji–Trost reactions were performed in water and air in the presence Pd/ Fe_3O_4 /PEI/rGO catalyst that contained 1.8 μ mol Pd and 7.2 μ mol PPh_3 .

Synergistic catalysis of a Pd species and base on a nonstructured solid surface has been recently reported in the Tsuji–Trost reaction.^[14] To test the potency of Pd/ Fe_3O_4 /PEI/rGO as a synergistic catalyst, we examined the Tsuji–Trost reaction between ethyl acetoacetate **1** and allyl ethyl carbonate **2** in water under optimized conditions. As shown in Table 1, the use of Pd/ Fe_3O_4 /PEI/rGO resulted in more than 99% yield of the total allylated products in half an hour (Table 1, entry 1). The yield of allylated products was 66% for Pd/rGO (the size of Pd is about 4 nm, which is close to the size of Pd on the Pd/ Fe_3O_4 /PEI/rGO; Figure S5b in the Supporting Information) without PEI (Table 1, entry 2). The Tsuji–Trost reaction that used Fe_3O_4 /PEI/rGO (Figure S5c in the Supporting Information) did not proceed (Table 1, entry 3). These results indicate that the tertiary amine on Pd/ Fe_3O_4 /PEI/rGO accelerates the Pd-catalyzed Tsuji–Trost reaction. To further prove this conclusion, the reaction with PEI/rGO was conducted by using Pd/rGO (Table 1, entry 4). The product yield was much lower than that for the reaction that used Pd/ Fe_3O_4 /PEI/rGO (Table 1, entry 1).

To further explore the scope of the synthetic applicability of the Pd/ Fe_3O_4 /PEI/rGO catalyst, other allylic substitution reactions were also examined in water and air under the optimized conditions. As shown in Table 2, nearly all of the allylic substitution reactions finished within three hours. In the reaction of 1,3-dicarbonyls, the results for Pd/rGO without PEI are also shown (Table 2). The Pd/ Fe_3O_4 /PEI/rGO catalyst showed good activity for the reaction of 1,3-diesters (Table 2, entries 19 and 21) and 1,3-diketone (Table 2, entries 23 and 25). Bulky alkyl esters, such as isopropyl acetoacetate, *tert*-butyl acetoacetate, and isobutyl acetoacetate, were also suitable substrates for this allylic alkylation process; they afforded the corresponding products in greater than 99% yields (Table 2, entries 7, 9, and 11). The high product yields indicate that the Pd/ Fe_3O_4 /PEI/rGO catalyst exhibits high catalytic activity for the bulky ester. For the phenyl keto ester, 81% yield of products was obtained (Table 2, entry 17). Interestingly, the ethyl-2-methyl-3-oxobutanoate with steric bulk also gave more than 99% product (Table 2, entry 15). For all 1,3-dicarbonyls used for comparison, Pd/ Fe_3O_4 /PEI/rGO showed higher product yields than Pd/rGO as well as other reported catalytic systems.^[14b]

Table 1. Tsuji–Trost reaction using various catalysts in H_2O and air.^[a]

Entry	Catalyst	t [h]	Yield [%]	TOF [h^{-1}] ^[b]	3/4 [%] ^[c]
1	Pd/ Fe_3O_4 /PEI/rGO	0.5	>99	>2200	40:60
2	Pd/rGO	1.0	66	733	30:70
3	Fe_3O_4 /PEI/rGO ^[d]	1.0	–	–	–
4	Fe_3O_4 /PEI/rGO ^[d] + Pd/rGO	1.0	73	811	15:85

[a] Reaction conditions: Pd catalyst (Pd: 1.8 mmol), PPh_3 (7.2 mmol), **1** (2.0 mmol), **2** (5.0 mmol), H_2O (3.0 mL), 100 °C. [b] TOF [h^{-1}] = $\frac{n(\text{product})}{n(\text{Pd}) \cdot t [h]}$. [c] Yields of isolated products determined by 1H and ^{13}C NMR spectroscopy. Tetramethylsilane was used as internal standard. [d] PEI/ Fe_3O_4 /rGO (Fe: 0.045 mmol) was used.

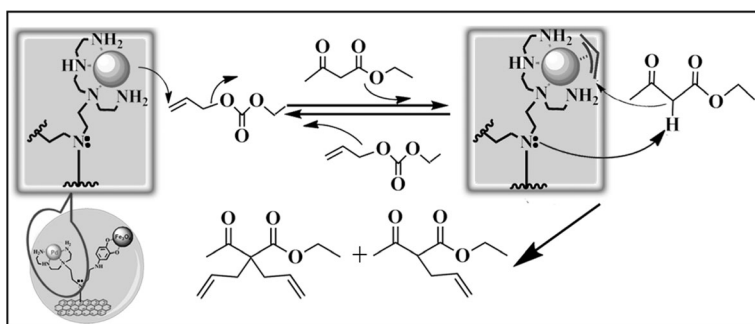
Table 2. The Tsuji–Trost reaction of various 1,3-dicarbonyl compounds with allyl ethyl carbonate in H_2O and air.^[a]

Entry	1,3-Dicarbonyl	Catalyst	t [h]	Mono/Di	Yield [%] ^[b]
1		Pd/ Fe_3O_4 /PEI/rGO	0.5	35:65	>99
2		Pd/ Fe_3O_4 /PEI/rGO	1.0	0:100	>99
3		Pd/rGO	1.0	13:87	68
4		Pd/ Fe_3O_4 /PEI/rGO	0.5	40:60	>99
5		Pd/ Fe_3O_4 /PEI/rGO	1.0	0:100	>99
6		Pd/rGO	1.0	30:70	66
7		Pd/ Fe_3O_4 /PEI/rGO	1.0	0:100	>99
8		Pd/rGO	1.0	2:98	59
9		Pd/ Fe_3O_4 /PEI/rGO	1.0	0:100	>99
10		Pd/rGO	1.0	13:87	26
11		Pd/ Fe_3O_4 /PEI/rGO	1.0	30:70	>99
12		Pd/rGO	1.0	13:87	53
13		Pd/ Fe_3O_4 /PEI/rGO	1.0	42:58	94
14		Pd/rGO	1.0	2:98	26
15		Pd/ Fe_3O_4 /PEI/rGO	1.5	–	>99
16		Pd/rGO	1.5	–	31
17		Pd/ Fe_3O_4 /PEI/rGO	4.0	0:100	81
18		Pd/rGO	4.0	0:100	43
19		Pd/ Fe_3O_4 /PEI/rGO	3.0	42:58	91
20		Pd/rGO	3.0	2:98	28
21		Pd/ Fe_3O_4 /PEI/rGO	3.0	42:58	88
22		Pd/rGO	3.0	2:98	26
23		Pd/ Fe_3O_4 /PEI/rGO	1.0	0:100	>99
24		Pd/rGO	1.0	0:100	43
25		Pd/ Fe_3O_4 /PEI/rGO	1.5	–	83
26		Pd/rGO	1.5	–	27

[a] Reaction conditions: Pd catalyst (Pd: 1.8 mmol), PPh_3 (7.2 mmol), **1** (2.0 mmol), **2** (5.0 mmol), H_2O (3.0 mL), 100 °C. [b] Yields of isolated products determined by 1H and ^{13}C NMR spectroscopy. Tetramethylsilane was used as internal standard.

Mechanistic studies

Generally, the mechanism of homogeneous Pd-mediated allylic alkylation is an allylic leaving group forming the η^3 -allylpalladium species, which reacts with various nucleophiles to furnish allylic compounds.^[7b,8b,c] To evaluate if the Pd/Fe₃O₄/PEI/rGO-mediated allylic alkylation involved the same mechanism, ¹H NMR spectroscopic experiments were conducted. Pd/Fe₃O₄/PEI/rGO exhibited a signal at $\delta = 3.60$ ppm, which was from PEI of Pd/Fe₃O₄/PEI/rGO. After treatment of Pd/Fe₃O₄/PEI/rGO with allyl ethyl carbonate **2**, two signals appeared at $\delta = 4.1$ ppm (α -H) and $\delta = 3.45$ ppm (β -H) that were enhanced relative to the signal at $\delta = 3.6$ ppm in the ¹H NMR spectrum (Figure S6b,c in the Supporting Information), thus indicating formation of the η^3 -allylpalladium species.^[15] On the basis of these observations and the different yields of allylated products using both Pd/rGO and Pd/Fe₃O₄/PEI/rGO, we conclude that Pd/Fe₃O₄/PEI/rGO-mediated allylic substitution in water proceeds through a mechanism close to that of homogeneous Pd catalysis. That is to say, in the Tsuji–Trost reaction, the PdNPs activate the allyl methyl carbonate to form a propylene/Pd nanocomposite while the tertiary amines simultaneously activate 1,3-dicarbonyls by abstraction of an α proton (Scheme 1).



Scheme 1. Possible mechanism of Pd/Fe₃O₄/PEI/rGO in the Tsuji–Trost reaction.

Recycling of the catalyst

Isolation, convenient recycling, and reuse of a catalyst are known to be crucial requirements to develop an efficient “green” system. For the recycling study, the Tsuji–Trost reaction was performed with ethyl acetoacetate **1** and allyl ethyl carbonate **2** and by maintaining the same reaction conditions as described above except that the recovered catalyst was used. In our systems, 30 reaction cycles were tested for the catalyst. After each run, the catalysts could be easily separated from the reaction mixture with the help of a magnet (Figure 2e, inset). Upon washing with ethyl acetate, the catalysts were directly used for the next round of reaction. As shown in Figure 3a, the catalyst can be reused 30 times and the yield still remains above 92%. The high recycle counts and yields have been discovered in our system for the first time and are very important for applications in industry. However, catalytic activities of other catalysts decrease very quickly after six cycles (Figure 3b). Similarly, the stability of the catalyst is highly desirable

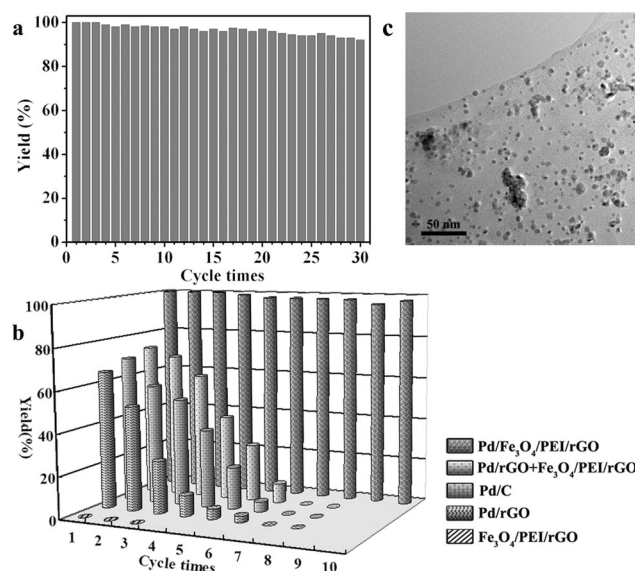


Figure 3. a) Reusability of Pd/Fe₃O₄/PEI/rGO for ethyl acetoacetate with allyl ethyl carbonate in water and air. b) TEM image of Pd/Fe₃O₄/PEI/rGO nanocomposites after 20 cycles. c) Recycling abilities of different nanocomposites in water and air (30 min).

for achieving high activity and catalyst reusability. To address this possibility, the evolution of Pd leaching was measured by means of inductively coupled plasma atomic emission spectroscopy (ICP–AES). After 20 cycles of reaction and magnetic separation of the catalyst, a total of 7.6% Pd remained in the liquid phase of water. Additionally, the morphologies of PdNPs of the recovered Pd/Fe₃O₄/PEI/rGO were examined by TEM (Figure 3c). The images indicate that the morphology and

size of PdNPs are highly dispersed on graphene surfaces after the twentieth reuse, which indicates that PEI can provide well-defined anchor sites for PdNPs and Fe₃O₄ NPs on the graphene surface and protect Pd nanoparticles from agglomeration. As a result, Pd/Fe₃O₄/PEI/rGO retains excellent catalytic activity during the recycling process. That could be the reason why the prepared catalyst has higher catalytic activity and stability than that reported previously.^[16]

Conclusion

We have developed a universal strategy for the preparation of strongly coupled Fe₃O₄ NPs and a noble-metal nanocatalyst on graphene sheets by employing PEI as the coupling linker. These ternary nanocomposites have a well-defined 2D morphology, controllable size, high dispersion of PdNPs and Fe₃O₄ NPs, and high specific surface area. We have demonstrated for

the first time that the present catalyst exhibits synergistic catalysis for the acceleration of the Tsuji–Trost reaction in water and air. More importantly, the noble-metal nanocatalyst on the magnetic support has a very low leaching loss and allows one to reach at least 92% yield in Tsuji–Trost catalysis over 30 cycling tests. All these characteristics are desirable in terms of cost and environmental protection. Since PEI can chelate various transition-metal cations, our work provides a general methodology for the preparation of other noble-metal/Fe₃O₄/PEI/rGO nanocomposites with high stability, high catalytic activity, and good magnetic recycling properties for industrial applications.

Experimental Section

Chemicals

Graphite flake, branched PEI, PdCl₂, DIB, [Fe(acac)₃] (acac = acetylacetonate; 99.9%), benzyl ether, oleylamine, and triphenylphosphine (PPh₃) were purchased from Sigma–Aldrich. Potassium permanganate (KMnO₄), sulfuric acid (H₂SO₄, 98%), hydrogen chloride (HCl, 37%), and hydrogen peroxide (H₂O₂, 30%) were obtained from Tianjin Med. All chemicals were used without further purification. The H₂O used throughout the entire experimental process was deionized H₂O. Graphene oxide (GO) was prepared from graphite flake powder according to a modified Hummers method,^[17] and Fe₃O₄ nanoparticles were prepared according to a previous work.^[18]

Instrumentation

TEM measurements were carried out with a JEM-2100 (200 kV) instrument under ambient conditions through the deposition of hexane or ethanol dispersions of the nanomaterials on amorphous carbon-coated copper grids. X-ray powder diffraction patterns of the particles were recorded using a Bruker AXS D8 Advance diffractometer with Cu_{Kα} radiation (λ = 1.5418 Å). X-ray photoelectron spectroscopy (XPS) measurements were performed using a PHI-5702 multifunctional spectrometer with Al_{Kα} radiation. Raman spectra were collected using a confocal microprobe Raman system (Renishaw, RM2000). Magnetic properties were studied using a Lakeshore 7404 high-sensitivity vibrating sample magnetometer (VSM) with fields up to 1.5 tesla at room temperature. IR spectra were recorded using a Nicolet FT-170SX spectrometer. TGA was carried out using a TA 2901 instrument under a nitrogen atmosphere at a heating rate of 10 °C min⁻¹ from 30 to 600 °C to determine the content of the PEI on the GO. ¹H and ¹³C NMR spectra were gathered using a JEOL ESC 400M instrument. Mass spectrometry was performed using a TPRACE DSO instrument.

Synthesis of DIB/PEI/rGO

PEI/rGO was prepared according to the literature with a little modification.^[19] GO (10 mg) was dispersed into deionized water (100 mL) to form a light brown dispersion by sonication for about 30 min, then a solution that contained PEI (1 g, M_n: 25 000) in distilled water (100 mL) was added. The reaction was maintained at 60 °C for 12 h. After that, the solvent was removed, and the product was separated by centrifugation and washed several times with ethanol and diethyl ether (1:4 v/v). The product was then re-dispersed into ethanol (100 mL). To prepare DIB/PEI/rGO, DIB (55 mg, 0.4 mmol) in ethanol (20 mL) was added dropwise into the

above dispersion. After stirring for another 12 h at room temperature, the solvent was evaporated by half under reduced pressure. The product was separated by centrifugation and washed three times with ethanol and diethyl ether (1:4 v/v) and then dispersed into ethanol (15 mL) as a stock solution.

Synthesis of Pd/PEI/rGO

Ethanol (40 mL) was added to the stock solution of DIB/PEI/rGO (3 mL, 2 mg GO) and sonicated for 10 min to obtain a suspension. The solution of PdCl₂ (4.0 mg, 0.023 mmol) in ethanol (5 mL) was added dropwise into the suspension and stirred for 2 h at room temperature to ensure the metal ions thoroughly bound to the N atoms of PEI. Then freshly dissolved NaBH₄ (5.2 mg, 0.14 mmol) in ethanol (2 mL) was added dropwise under an N₂ atmosphere into the above solution over 10 min and stirred for another 2 h. The raw product was centrifuged after adding hexane (40 mL) and washed three times with excess amounts of ethanol and hexane. The resulting solid was then redispersed into ethanol and chloroform (40 mL, 2:1 v/v).

Synthesis of Pd/Fe₃O₄/PEI/rGO

Fe₃O₄ NPs (4 mg) in a fresh mixture of ethanol and chloroform (4 mL, 2:1 v/v) was added into as-prepared Pd/PEI/rGO stock solution and stirred overnight at room temperature. The product was precipitated by adding hexane and collected by means of an exogenous magnet. The residual solid was washed with hexane three times. Finally, the solid product was obtained by vacuum drying under an N₂ atmosphere.

Pd/Fe₃O₄/PEI/rGO catalyst for the Tsuji–Trost reaction

For the Tsuji–Trost reaction, 1,3-dicarbonyl (2.0 mmol), allyl ethyl carbonate (5.0 mmol), PPh₃ (7.2 μmol), and H₂O (3 mL) were used. The amount of catalyst used in each reaction was 10 mg (Pd: 1.8 μmol), and the reaction mixture was heated under reflux conditions at 100 °C under air. The reaction process was monitored by thin layer chromatography (TLC). After completion of the reaction, the mixture was cooled to room temperature and separated by magnetic separation. The residual mixture was washed with ethyl acetate (3 × 1 mL). The product was separated by column chromatography and determined by ¹H and ¹³C NMR spectroscopy and MS. After the first cycle of the reaction, another 3 mL of H₂O, 7.2 μmol of PPh₃, and the corresponding substrates were added for the next cycle.

Acknowledgements

The work was supported by the National Natural Science Foundation of China (21271093), the NCET (13-0262), and the Fundamental Research Funds for the Central Universities (Izujbky-2013-56 and Izujbky-2014-k06).

Keywords: graphene · palladium · nanoparticles · synergistic catalysis · Tsuji–Trost reaction

- [1] a) M. Lamblin, L. Nassar-Hardy, J. C. Hierso, E. Fouquet, F. X. Felpin, *Adv. Synth. Catal.* **2010**, *352*, 33–79; b) S. U. Son, Y. J. Jang, J. Park, H. B. Na, H. M. Park, H. J. Yun, J. Lee, T. Hyeon, *J. Am. Chem. Soc.* **2004**, *126*, 5026–5027; c) S. W. Kim, M. Kim, W. Y. Lee, T. Hyeon, *J. Am. Chem. Soc.* **2002**, *124*, 7642–7643; d) H. M. Chen, C. K. Chen, R. S. Liu, L. Zhang, J. J.

- Zhang, D. P. Wilkinson, *Chem. Soc. Rev.* **2012**, *41*, 5654–5671; e) Z. J. Han, F. Qiu, R. Eisenberg, P. L. Holland, T. D. Krauss, *Science* **2012**, *338*, 1321–1324; f) E. Formo, Z. M. Peng, E. Lee, X. M. Lu, H. Yang, Y. N. Xia, *J. Phys. Chem. C* **2008**, *112*, 9970–9975; g) J. H. He, I. Ichinose, T. Kunitake, A. Nakao, Y. Shiraiishi, N. Toshima, *J. Am. Chem. Soc.* **2003**, *125*, 11034–11040; h) S. H. Joo, S. J. Choi, I. Oh, J. Kwak, Z. Liu, O. Terasaki, R. Ryoo, *Nature* **2001**, *412*, 169–172.
- [2] Z. Jin, D. Nackashi, W. Lu, C. Kittrell, J. M. Tour, *Chem. Mater.* **2010**, *22*, 5695–5699.
- [3] a) K. Köhler, R. G. Heidenreich, J. G. E. Krauter, J. Pietsch, *Chem. Eur. J.* **2002**, *8*, 622–631; b) G. Z. Hu, F. Nitzte, T. Sharifi, H. R. Barzegar, T. Wågberg, *J. Mater. Chem.* **2012**, *22*, 8541–8548; c) Y. R. Choi, M. S. Gu, J. N. Park, H. K. Song, B. S. Kim, *Adv. Energy Mater.* **2012**, *2*, 1510–1518; d) P. H. Li, L. Wang, L. Zhang, G. W. Wang, *Adv. Synth. Catal.* **2012**, *354*, 1307–1318; e) B. H. San, S. Kim, S. H. Moh, H. Lee, D. Y. Jung, K. K. Kim, *Angew. Chem.* **2011**, *123*, 12130–12135; *Angew. Chem. Int. Ed.* **2011**, *50*, 11924–11929; f) R. M. Crooks, M. Q. Zhao, L. Sun, V. Chechik, L. K. Yeung, *Acc. Chem. Res.* **2001**, *34*, 181–190; g) S. Mandal, D. Roy, R. V. Chaudhari, M. Sastry, *Chem. Mater.* **2004**, *16*, 3714–3724; h) A. J. Amali, R. K. Rana, *Chem. Commun.* **2008**, *35*, 4165–4167.
- [4] a) S. Shylesh, V. Schünemann, W. R. Thiel, *Angew. Chem.* **2010**, *122*, 3504–3537; *Angew. Chem. Int. Ed.* **2010**, *49*, 3428–3459; b) J. Liu, S. Z. Qiao, Q. H. Hu, G. Q. Lu, *Small* **2011**, *7*, 425–443.
- [5] a) X. Huo, J. Liu, B. D. Wang, H. L. Zhang, Z. Y. Yang, X. G. She, P. X. Xi, *J. Mater. Chem. A* **2013**, *1*, 651–656; b) C. V. Rao, C. R. Cabrera, Y. Ishikawa, *J. Phys. Chem. C* **2011**, *115*, 21963–21970.
- [6] R. N. Butler, A. G. Coyne, *Chem. Rev.* **2010**, *110*, 6302–6337.
- [7] a) J. Tsuji, *Acc. Chem. Res.* **1969**, *2*, 144–152; b) B. M. Trost, M. L. Crawley, *Chem. Rev.* **2003**, *103*, 2921–2943.
- [8] a) Y. Uozumi, K. Shibatomi, *J. Am. Chem. Soc.* **2001**, *123*, 2919–2920; b) Y. Uozumi, *Pure Appl. Chem.* **2007**, *79*, 1481–1489; c) F. X. Felpin, Y. Landais, *J. Org. Chem.* **2005**, *70*, 6441–6446.
- [9] a) C. J. Xu, K. M. Xu, H. W. Gu, R. K. Zheng, H. Liu, X. X. Zhang, Z. H. Guo, B. Xu, *J. Am. Chem. Soc.* **2004**, *126*, 9938–9939; b) J. Xie, C. J. Xu, N. Kohler, Y. L. Hou, S. H. Sun, *Adv. Mater.* **2007**, *19*, 3163–3166.
- [10] A. J. Amali, R. K. Rana, *Green Chem.* **2009**, *11*, 1781–1786.
- [11] a) T. Yang, C. Shen, Z. Li, H. Zhang, C. Xiao, S. Chen, Z. Xu, D. Shi, J. Li, H. Gao, *J. Phys. Chem. B* **2005**, *109*, 23233–23236; b) J. Xie, K. Chen, H. Lee, C. Xu, A. R. Hsu, S. Peng, X. Chen, S. Sun, *J. Am. Chem. Soc.* **2008**, *130*, 7542–7543.
- [12] S. Li, D. Q. Wu, C. Cheng, J. Z. Wang, F. Zhang, Y. Z. Su, X. L. Feng, *Angew. Chem.* **2013**, *125*, 12327–12331.
- [13] M. Y. Zhu, G. W. Diao, *J. Phys. Chem. C* **2011**, *115*, 24743–24749.
- [14] a) H. Noda, K. Motokura, A. Miyaji, T. Baba, *Angew. Chem.* **2012**, *124*, 8141–8144; *Angew. Chem. Int. Ed.* **2012**, *51*, 8017–8020; b) H. Noda, K. Motokura, A. Miyaji, T. Baba, *Adv. Synth. Catal.* **2013**, *355*, 973–980.
- [15] H. Kinoshita, H. Shinokubo, K. Oshima, *Org. Lett.* **2004**, *6*, 4085–4088.
- [16] T. Mitsudome, K. Nose, K. Mori, T. Mizugaki, K. Ebitani, K. Jitsukawa, K. Kaneda, *Angew. Chem.* **2007**, *46*, 3288–3290.
- [17] W. S. Hummers, R. E. Offeman, *J. Am. Chem. Soc.* **1958**, *80*, 1339.
- [18] Z. C. Xu, C. M. Shen, Y. L. Hou, H. J. Gao, S. H. Sun, *Chem. Mater.* **2009**, *21*, 1778–1780.
- [19] a) D. S. Yu, L. M. Dai, *J. Phys. Chem. Lett.* **2010**, *1*, 467–470; b) X. H. Zhou, Z. X. Chen, D. H. Yan, H. B. Lu, *J. Mater. Chem.* **2012**, *22*, 13506–13516.

Received: March 11, 2014

Published online on July 22, 2014